

# Measurement of the rotational distribution for the OD product from the reaction $\text{ND}_3^+ + \text{D}_2\text{O} \rightarrow \text{ND}_4^+ + \text{OD}$ under translationally thermal conditions

Richard J. Green and Richard N. Zare

*Department of Chemistry, Stanford University, Stanford, California 94305-5080*

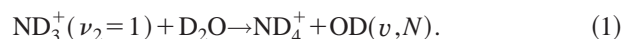
(Received 29 July 1996; accepted 10 April 1997)

The state-to-state ion-molecule reaction  $\text{ND}_3^+(\nu_2=1) + \text{D}_2\text{O} \rightarrow \text{ND}_4^+ + \text{OD}(v=0, N)$  is investigated. A slowly flowing, 2:1 mixture of  $\text{ND}_3$  and  $\text{D}_2\text{O}$  at a total pressure of 50 mTorr is irradiated with a two-color sequence of laser pulses that prepares  $\text{ND}_3^+$  in either the  $\nu_2=1$  umbrella bending mode or the ground vibrational state by  $1+1'+1$  resonance-enhanced multiphoton ionization via the  $\text{ND}_3 \tilde{A}$  and  $\tilde{B}$  states. After a delay of 200 ns to allow product buildup, the rotational distribution of the  $\text{OD}(v=0)$  product is measured by recording the  $\text{OD } A^2\Sigma^+ - X^2\Pi$  laser-induced fluorescence spectrum on the (1,1) band following excitation of the (1,0) band. Rotational distributions are presented for the  ${}^2\Pi_{3/2}$  and  ${}^2\Pi_{1/2}$  fine-structure states of the OD product for the reaction of the vibrationally excited reactant ion; for the experimentally difficult case of the reactant ion in the ground state, a rotational distribution is presented for the  ${}^2\Pi_{3/2}$  fine-structure state of the OD product. For the case of the reaction with excited  $\text{ND}_3^+$ , the relative rotational populations are fit to a Boltzmann distribution to yield temperatures of  $990 \pm 30$  K and  $890 \pm 70$  K for the OD  ${}^2\Pi_{3/2}$  and  ${}^2\Pi_{1/2}$  fine-structure components, respectively. For the ground state ion, such a fit yields a temperature of  $700 \pm 100$  K for the OD  ${}^2\Pi_{3/2}$  fine-structure component. The results are compared to an RRKM-type model that predicts a rotational distribution of 800 K, and 940 K for the reaction of ion with  $\nu_2=0$  and  $\nu_2=1$ , respectively. The excellent agreement is evidence for reaction through a long-lived complex. © 1997 American Institute of Physics. [S0021-9606(97)02127-2]

## I. INTRODUCTION

Ion-molecule reactions have been studied in great detail for numerous systems using various techniques.<sup>1,2</sup> It is very difficult, however, to study such reactions in a detailed manner without creating an ion beam in which the translational energies are not thermal. The possibility of studying state-to-state ion-molecule reactions under translationally thermal conditions by coupling resonance-enhanced multiphoton ionization (REMPI) to laser-induced fluorescence (LIF) in a bulb has been suggested for some time.<sup>3</sup> The advantage of using REMPI is that it is possible to produce ions in specific vibrational energy levels.<sup>4</sup> After the ions are produced, they can react with neutral molecules that are present. LIF detection offers two advantages: LIF can be used to detect the products with rotational resolution,<sup>5</sup> and the LIF laser beam can be overlapped with the REMPI beam, eliminating the need for an ion beam to localize the reaction. Such an experiment was carried out on the charge-transfer reaction of  $\text{DBr}^+$  with  $\text{HBr}$  and yielded absolute state-to-state thermal rate constants.<sup>6</sup>

In this work we present a study of an ion-molecule reaction in which deuterium atom exchange occurs. For the reaction system chosen, we can select the vibrational level of the reactant ion and observe the rotational distribution of a neutral product. The reaction is



The results reported here are for the reaction in which the ion has one quantum of excitation in the symmetric bend or um-

rella mode, denoted by  $\nu_2$ , as well as for the ground vibrational state of the ion. The hydrogen isotope analog of this reaction



has been studied previously by several groups.<sup>7-11</sup> Kemper *et al.*<sup>11</sup> found rate constants on the order of  $2.3 \times 10^{-10}$  cm<sup>3</sup>/s at internal energies where reaction (2a) is the major channel, up to  $7 \times 10^{-10}$  cm<sup>3</sup>/s at internal energies where 98% of the reaction goes by channel (2b). The rate constant for channel (2a) was found to decrease as a function of internal energy. None of these studies, however, involved vibrational state selection of the  $\text{NH}_3^+$  ion and determination of the rotational distribution of the OH product. We study the deuterated reaction because of the short predissociation lifetime of the  $\tilde{A}$  state of ammonia, which is an intermediate in our ionization process. Deuteration causes this lifetime to be longer, owing to the zero-point energy difference and the lower tunneling probability of deuterium. The water is also deuterated to prevent isotope exchange between the neutral gases in the mixture.

Our study allows us to measure the rotational distribution of the OD product that results from the reaction of the ion prepared in a specific vibrational energy state. In the current work we prepare the ion with  $\nu_2=0,1$ . We fit our rotational distribution to a temperature to understand energy partitioning in the reaction. Ion-molecule reactions proceeding at thermal energies are generally believed to proceed through long-lived complexes that would lead to statistical

energy distributions in the products. We compare our results to a simple model of such a statistical distribution and find good agreement.

## II. EXPERIMENT

The experimental apparatus has been described previously,<sup>6</sup> but because substantial changes have occurred the apparatus merits some additional explanation.

The reaction chamber is a stainless steel thermal gas cell. There are no molecular beams and hence no spatial separation of reactants and products. Before use, the chamber is exhausted through a liquid nitrogen trap to  $10^{-7}$ – $10^{-6}$  Torr by means of a 3-in diffusion pump (EO2, Edwards). The reactant gases are premixed so that the ratio of the concentrations of the gases does not change during an experiment. The  $\text{D}_2\text{O}$  (99.9% isotopically pure, Aldrich) is purified of dissolved gases by three freeze-pump-thaw cycles; the  $\text{ND}_3$  (99% isotopically pure, Cambridge Isotopes) is used without further purification. The mixing cell is filled with a mixture of  $\text{ND}_3$  and  $\text{D}_2\text{O}$  in the ratio 2:1 as measured by a capacitance manometer (Model 122AA, MKS Instruments). Gas from the mixing cell is leaked into the reaction cell and simultaneously pumped out so that new gas always flows into the reaction cell at a slow constant rate. The reaction cell is maintained at  $50 \pm 1$  mTorr total gas pressure, as monitored by a second capacitance manometer (Model 122AA MKS Instruments).

State-selective ionization of ammonia via (2+1) REMPI through the  $\tilde{C}'$  and  $\tilde{B}$  states is well known and produces ions with good state selectivity.<sup>4,12,13</sup> The lack of spatial separation of our reactants, however, precludes us from using such a direct method because  $\text{D}_2\text{O}$  is easily photolyzed by a two-photon absorption at wavelengths required to use such a scheme. We have, in fact, observed OD produced from such a photolysis. If such a method of ionizing the  $\text{ND}_3$  were employed, we would have no method to differentiate the reactive OD signal from the OD produced by photolysis. We use a two-color ionization scheme to avoid this difficulty.

Ground-state  $\text{ND}_3$  is first excited to the  $\tilde{A}$  ( $\nu_2 = 1$ ) state via the  $P(4)$  line at 211.35 nm for  $\nu_2 = 1$  and to the  $\tilde{A}$  ( $\nu_2 = 0$ ) state via the unresolved  $P$  branch (at approximately  $J = 3$ ) at 214.16 nm for  $\nu_2 = 0$ ; it is subsequently excited to the  $\tilde{B}$  state with 578.75 nm laser light for  $\nu_2 = 1$  and 579.33 nm laser light for  $\nu_2 = 0$ ; a second UV photon ionizes the molecule. The laser light is generated as follows: The third harmonic of a Nd:YAG laser (GCR-3, Spectra-Physics) pumps a dye laser (PDL-3, Spectra-Physics) containing LD425 (Exciton). The output of the dye laser is frequency doubled through a 70 degree  $\beta$ -barium borate (BBO) crystal to generate the 211.35 and 214.16 nm laser light (hereafter referred to as the UV ionization laser light). The residual second harmonic of the same Nd:YAG laser is used to pump a second dye laser (PDL-1, QuantaRay) containing Rhodamine 610 (Exciton); this laser is the source of the 578.75 and 579.33 nm laser light (hereafter referred to as the visible ionization laser light). The UV beam has an output of

about 1 mJ and is telescoped and irised to a spot size of 2–3 mm in the case of  $\nu_2 = 1$ . In the case of  $\nu_2 = 0$ , the UV beam is focused with a 500 mm lens to drive this more difficult transition. The signal to noise ratio in results for  $\nu_2 = 0$  are unavoidably worse because of the difficulty in driving this transition. The visible beam is sent through a delay line so that its arrival time at the reaction cell overlaps with that of the UV beam. The polarization of the visible beam is changed from vertical to horizontal by means of two consecutive turning prisms on a single mount so that it corresponds with the horizontal polarization of the UV beam. The beams counterpropagate into the reaction chamber and the overlap is optimized to give maximum ion signal. A chopper (model 192, EG&G) blocks the visible light. The Nd:YAG laser is triggered from a circuit that takes input from a photodiode in the chopper. The lasers are triggered in such a way that the Nd:YAG fires at 10 Hz, but the visible laser is blocked by every other shot. This configuration allows us to eliminate any interfering reaction pathways initiated only by the UV laser. The ions produced are monitored so that product signal can be normalized to the amount of reactant produced. A 90 V pulse is applied to a metal plate at a time sufficiently late so as not to interfere with the detection of reactive products. The resultant ion signal collected with a parallel plate is averaged by a boxcar (model 162, PAR) whose output is digitized by an analog-to-digital converter (DT2817, Data Translation), hereafter referred to as the AD converter, and then to a 486 computer (HD), hereafter referred to as the PC.

The OD product is detected by LIF 200 ns after the ionizing lasers are fired. The OD is excited via the (1,0) band of the  $A-X$  transition and fluorescence is detected from the (1,1) band. The excitation light is produced by the doubled output of a third dye laser (PDL-1, QuantaRay) containing a mixture of Rhodamine 610 (Exciton) and Rhodamine 590 (Exciton) and pumped by the second harmonic of a second Nd:YAG laser (DCR-1, QuantaRay). The output of this dye laser passes through a doubling autotracker (WEX-1, QuantaRay) containing a 68 degree potassium dihydrogen phosphate (KDP) crystal. The doubled light is separated by means of an absorption filter to minimize beam walk caused by dispersion as the laser wavelength is scanned. The LIF beam is irised, but kept large enough to encompass entirely the UV ionizing beam. The LIF beam is combined with the visible ionizing beam by means of a dichroic mirror before it enters the chamber. The chamber is equipped with Brewster's angle windows and anodized baffles to reduce scattered light. The laser power is kept high to ensure saturation of the OD transition: the estimated laser fluence is  $2500 \mu\text{J}/\text{cm}^2$ , within the regime of complete saturation.<sup>14</sup> The power is monitored from a back reflection by a pyroelectric detector (J4-09, Molelectron) as the laser is scanned. The output of the detector is averaged on a boxcar (SR250, SRS) and sent to the AD converter which feeds the PC.

The fluorescence from the (1,1) transition of OD is collected by a 2 in diameter f1 lens system and a spherical mirror on the opposite side. The fluorescence is imaged onto the  $12 \times 12$  mm cathode of a gated photomultiplier tube

(PMT) (R943-02, Hamamatsu) with a gated D-type socket assembly (C1392-02, Hamamatsu). Before reaching the PMT the light passes through an interference filter (310, Corion). The wavelength-dependent transmission profile of the entire collection system has been measured *in situ* following the method of Bischel *et al.* as described below.<sup>15</sup> The gate on the photomultiplier is adjusted to block out the direct scattering of the LIF laser. The fluorescence signal is integrated for 1.5  $\mu\text{s}$  using an AD converter (2249W, LeCroy) and a gate and delay generator (2323A, LeCroy) and sent by a CAMAC crate (model 1502, Kinetic Systems) to the PC.

We conducted measurements on the wavelength dependence of our fluorescence detection system. The chamber was filled with 150 Torr of hydrogen gas. A dye laser was stepped in 1 nm increments over three overlapping ranges from 259–281 nm. The range from 259–272 nm was covered by means of coumarin 500 (Exciton) laser dye and an 83 degree KDP crystal, the range from 270–274 nm by coumarin 500 and a 74 degree KDP crystal, and the range from 270–281 nm by base-shifted fluorescein 548 (Exciton) and a 74 degree KDP crystal. The coumarin was pumped with the third harmonic of a YAG and the fluorescence from the second harmonic. The laser power was monitored from a back reflection using a pyroelectric detector (J4-09, Moletron). Multiple scans were done over each wavelength range. The Raman scattering was observed by integrating the output of the PMT with a digitizing oscilloscope (TDS 620, Tektronics). The scans were normalized to one another by means of their overlapping regions. The positions of the interference filter, the PMT, and irises governing the laser position through the chamber, were kept constant throughout these measurements and the reactive experiments. Pressure and power dependencies were done on the Raman intensity; each was found to be linear, as expected. The measurements were repeated with argon in place of hydrogen to make a slight correction for the Rayleigh scattering. From these measurements we were able to obtain a wavelength-dependent transmission profile from 295–328 nm by following the method of Bischel *et al.*<sup>15</sup>

### III. RESULTS AND ANALYSIS

The experiments were run at 50 mTorr of total gas pressure and with a delay between the ionization and LIF lasers of 200 ns. We conducted pressure-dependence studies from 30 to 100 mTorr to check for the effects of rotational relaxation and quenching. Within our error bars we observed no pressure dependence of the OD rotational distribution.

For the actual experiments the laser was scanned over nine overlapping regions between 287.2 and 291.0 nm. Separating the scans in this manner shortens the time of an experimental run, which ensures that conditions do not change significantly during any individual run. The regions overlap one another so that the average results for each scan region can be normalized to the average results of its neighboring regions. Each peak in the OD spectrum was assigned according to Sastry and Rao<sup>16</sup> and integrated numerically for the signal with the visible ionization laser blocked and un-

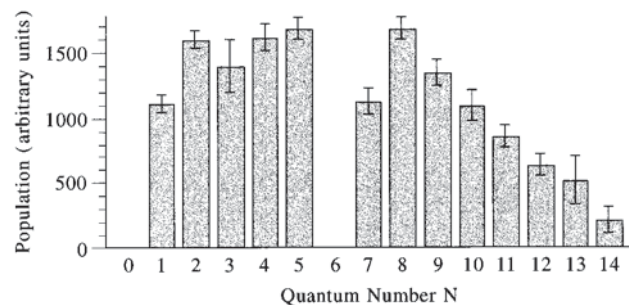


FIG. 1. Product OD ( ${}^2\Pi_{3/2}, v=0$ ) rotational distribution from the reaction  $\text{ND}_3^+(\nu_2=1) + \text{D}_2\text{O}$ . The relative population for  $N=6$  is not shown because no unblended transitions originating from this level were resolved. The error bars represent the 95% confidence level.

blocked. The average laser power and average ion signal for each peak were also calculated for both of these conditions. The peak areas were subtracted to yield a peak area for the reactive signal; we refer to the result of this subtraction as the reactive signal. We refer to the peak areas measured with the visible ionization laser blocked as the interference signal.

Both signals were normalized by the square root of the laser power. For saturated signal the peak height should be independent of the laser power, but the width should vary as the square root; therefore the area should vary as the square root.<sup>17–19</sup> The reactive signal was normalized by the difference between the ion signal with the visible laser blocked and unblocked. The interference signal was normalized by the ion signal with the laser blocked. Both signals were then normalized by the total corrected reactive signal for each scan. The scans for each region were averaged together and then normalized to each other by the ratios of their overlapping peaks.

Populations shown in Figs. 1–3 were calculated from these normalized and corrected line areas as follows. Each line was divided by the square root<sup>18,19</sup> of the appropriate Einstein  $B$  coefficient.<sup>20</sup> A fluorescence normalization factor was calculated for each line by taking into account all the possible ways the excited-state level can fluoresce within the (1,1) band, the Einstein  $A$  coefficients<sup>20</sup> of those lines, and

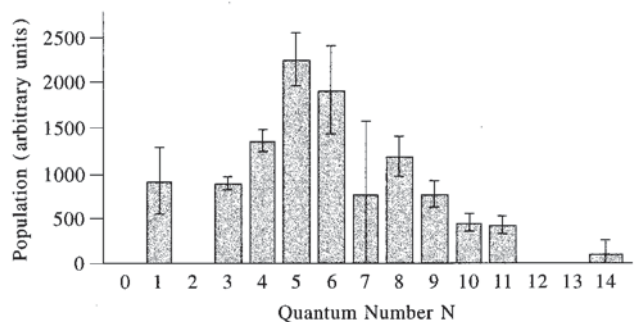


FIG. 2. Product OD ( ${}^2\Pi_{1/2}, v=0$ ) rotational distribution from the reaction  $\text{ND}_3^+(\nu_2=1) + \text{D}_2\text{O}$ . The relative populations for  $N=2, 12$ , and  $13$  are not shown because no unblended transitions originating from this level were resolved. The error bars represent the 95% confidence level.

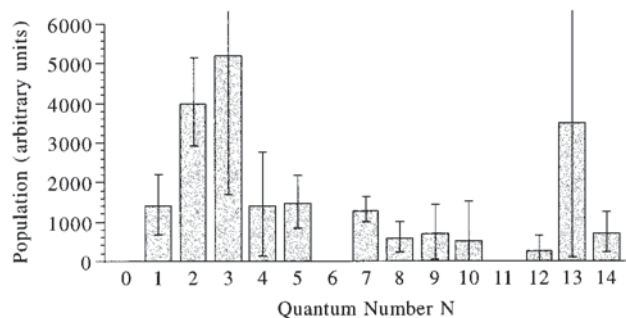


FIG. 3. Product OD ( ${}^2\Pi_{3/2}$ ,  $v=0$ ) rotational distribution from the reaction  $\text{ND}_3^+(\nu_2=0) + \text{D}_2\text{O}$ . The relative population for  $N=6$  is not shown because no unblended transitions originating from this level were resolved. The error bars represent the 95% confidence level.

the measured transmission efficiency at the appropriate wavelength where the wavelength for each line was assigned according to Clyne, Coxon, and Fat.<sup>21</sup> Although lines are discernible for rotational levels up to  $N=18$ , the signal to noise for many of the high  $N$  lines is not good enough to extract a reliable population. In addition, populations are not used for levels that can only be derived from blended lines. In the case of the reaction of  $\text{ND}_3^+(\nu_2=1)$  distributions are reported for both fine-structure states of the OD product. In the case of the reaction of  $\text{ND}_3^+(\nu_2=0)$  only a distribution for the  ${}^2\Pi_{3/2}$ , the fine-structure state, is reported, owing to the fact that relative errors for populations derived from the  ${}^2\Pi_{1/2}$  fine-structure state were greater than 1. The large relative errors for the product of the reaction of  $\text{ND}_3^+(\nu_2=0)$  owe to the necessity of focusing the UV ionization laser and increasing the interference signal. The spin-orbit splitting for  $N=1$  calculated by the difference in energy of the  $P_1(1)$  and  $P_{12}(1)$  lines of Clyne, Coxon, and Fat is  $130 \text{ cm}^{-1}$ .

In deriving a population we assume that there is no alignment of the OD product. Although the ammonia-d3 is ionized with linear polarized light we do not resolve the  $K$  quantum number in the ionization of the ammonia-d3. Also, the  $\text{D}_2\text{O}$  is isotropic. In principle, it is still possible to have a slight alignment of our OD product, but we expect any such alignment to be washed out. Because we do not resolve the satellite branches of the OD, it is not possible to separate any alignment effects from electron-orbital alignment without polarization experiments that would be particularly difficult for this experiment on account of the low signal to noise of an individual scan. The main  $Q$  branches for either spin-orbit state originate from different  $\Lambda$ -doublet levels than the main  $R$  and  $P$  branches do; thus the difficulty in separating the effect of any possible alignment from possible electronic alignment. To correct for the slight polarization effect of our excitation and detection geometry, populations were derived from the addition of all three branches, or by doubling the population of either the  $R$  or  $P$  branch and adding it to the  $Q$  branch, when possible. This correction is valid in the classical limit of high  $N$ .

Figure 4 shows the resulting populations as Boltzmann fits to straight lines using a least-squares linear regression to

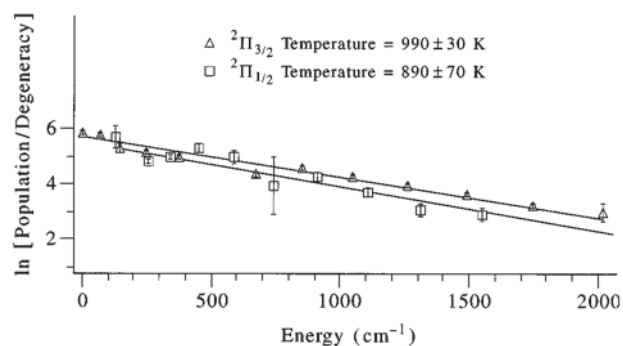


FIG. 4. Boltzmann plot of product OD ( $v=0$ ) rotational distributions from the reaction  $\text{ND}_3^+(\nu_2=1) + \text{D}_2\text{O}$  and fits to least squares linear regressions. The error bars represent the 95% confidence level.

obtain rotational temperatures for the reaction of  $\text{ND}_3^+(\nu_2=1)$ , and Fig. 5 does the same for the reaction of  $\text{ND}_3^+(\nu_2=0)$ . There is no *a priori* reason to expect that these distributions should necessarily correspond to a temperature; nevertheless, such a fit is a convenient method for arriving at an average rotational energy of the distribution. Each spin-orbit state of both the reactive and interference populations is fit independently. For the reactive population, the fits yield temperatures of  $990 \pm 30 \text{ K}$ , and  $890 \pm 70 \text{ K}$ , for the OD  ${}^2\Pi_{3/2}$  and  ${}^2\Pi_{1/2}$  fine-structure components of the reaction of  $\text{ND}_3^+(\nu_2=1)$ , respectively. The fits of the interfering signals yield  $1170 \pm 20 \text{ K}$  and  $1180 \pm 60 \text{ K}$ , respectively. For the reaction of the ground-state ion the fits for OD  ${}^2\Pi_{3/2}$  yielded  $700 \pm 100 \text{ K}$  for the reactive population and  $800 \pm 100 \text{ K}$  for the interference population.

#### IV. DISCUSSION

We have obtained rotational distributions of the OD product from reaction (1) under translationally thermal conditions. In this reaction the  $\text{ND}_3$  is state-selectively ionized via a two-color ionization scheme resulting in  $\text{ND}_3^+$  with one or zero quanta in the  $\nu_2$  mode. OD is detected by means of laser-induced fluorescence. Data are acquired with a shot-to-shot subtraction scheme to eliminate interference.

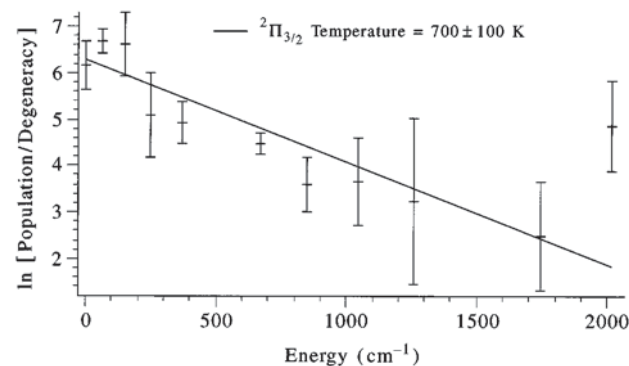


FIG. 5. Boltzmann plot of product OD ( ${}^2\Pi_{3/2}$ ,  $v=0$ ) rotational distribution from the reaction  $\text{ND}_3^+(\nu_2=0) + \text{D}_2\text{O}$  and fits to least squares linear regressions. The error bars represent the 95% confidence level.

## A. Nature of the interfering signal

It is worth considering briefly the nature of the interfering signal, i.e., the LIF signal that is observed when the visible ionization laser is blocked so that the OD detected must be produced by the UV ionization beam. It should first be noted that some of the interference signal persists in a control experiment in which there is no ammonia-d3 in the reaction cell, contrary to what is observed for the reactive signal. This observation indicates that at least some of the interference signal is the product of the photolysis of  $\text{D}_2\text{O}$ . 211 nm light is not energetic enough to photolyze  $\text{D}_2\text{O}$  with one photon;<sup>22,23</sup> it stands to reason that this interference contribution is a two-photon photolysis of  $\text{D}_2\text{O}$ .

When ammonia-d3 is present in the cell as well as  $\text{D}_2\text{O}$ , the interference signal is greatly enhanced, and, of course, the reactive signal appears. We suggest that the additional interference signal arises from an ion-molecule reaction in which the ions are the product of (1+1) REMPI through the  $\tilde{A}$  state of ammonia-d3. It should be noted that we were able to observe  $v=1$  product in the interfering signal via the (2,1) band of the OD  $A-X$  system, but that no such signal was observed in the simultaneous reactive spectrum; it is reasonable to infer that this  $v=1$  signal comes from photolysis of the  $\text{D}_2\text{O}$  only. The interference signal in the reaction of  $\text{ND}_3^+(\nu_2=0)$  is much greater than the interference in the reaction of  $\text{ND}_3^+(\nu_2=1)$  due to the need to focus the UV beam harder. This harder focusing promotes 1+1 REMPI through the  $\tilde{A}$  state of ammonia-d3. Because the interference signal is cancelled on a shot-by-shot subtraction basis, we need not concern ourselves further about its origin, and we can focus our attention instead on the reactive signal.

## B. Discussion of the reactive signal

For comparison with the experimental results, we construct a statistical model for the rotational temperature of the reactive signal based on the assumption that the reactive process goes on for a duration sufficiently long for the available energy to randomize itself among the various modes. Such reactions are often described as proceeding through long-lived complexes. In this context the characterization of a complex as ‘‘long-lived’’ should be understood to be relative to the amount of time required for the redistribution of internal energy. We first discuss the energetics of reaction (1) and then introduce the statistical model itself.

The 0.30 eV value of the exothermicity of reaction (1) was obtained from a series of quantum mechanical calculations with the CBS-APNO model chemistry<sup>24–28</sup> using the Gaussian computer program.<sup>29</sup> The analogous CBS-APNO calculation on reaction (2a) yielded an exothermicity of 0.26 eV in good agreement with the experimental value of 0.25 eV.<sup>11</sup> Table I shows the heats of atomization of the reactants and products obtained from the Gaussian calculations. For the case of reaction (1) with reactant  $\text{ND}_3^+(\nu_2=1)$  the 0.086 eV energy of vibrational excitation<sup>4</sup> of the reactant ion was added to the exothermicity of reaction.

TABLE I. Thermochemical data.

Species	0 K energy of atomization (hartrees) from CBS-APNO <sup>a</sup> Gaussian <sup>b</sup> calculations	0 K energy of atomization (eV)
$\text{ND}_3^+$	–56.161 33	–1528.240
$\text{D}_2\text{O}$	–76.416 96	–2079.428
OD	–75.725 60	–2060.615
$\text{ND}_4^+$	–56.863 64	–1547.351
Exothermicity (eV)		–0.30
$\text{NH}_3^+$	–56.151 98	–1527.985
$\text{H}_2\text{O}$	–76.410 61	–2079.255
OH	–75.723 06	–2060.546
$\text{NH}_4^+$	–56.849 26	–1546.959
Exothermicity (eV)		–0.26

<sup>a</sup>References 24–28.

<sup>b</sup>Reference 29.

Rice, Rampsperger, Kassel, and Marcus (RRKM) theory<sup>30–40</sup> presents an expression for the statistical decay of an energized molecule, which in our case corresponds to the possible long-lived complex:

$$k = \frac{W(E)}{hN(E)}, \quad (3)$$

in which  $W$  is the sum of states at the transition state,  $N$  is the density of states of the reactant molecule,  $E$  is the internal energy of the energized reactant molecule, and  $h$  is Planck’s constant. In the case of a loose transition state, i.e., one in which it is difficult to locate the geometry at which a bottleneck for reaction occurs, the transition state structure can be variationally optimized from a product-like structure.

Forst and Prasil<sup>36,38</sup> derived a method for estimating the density and sum of states of a molecule (or of a transition state) given an expression for the partition function. We follow the simpler notation of Robinson and Holbrook.<sup>37</sup> The benefit of this method is that it yields directly an expression for the temperature of the transition state. The partition function of a molecule can be written as the Laplace transform of the density of states:

$$Q(\beta) = \int_0^\infty N(E) \exp(-\beta E) dE, \quad (4)$$

where  $\beta = 1/kT$ ,  $k$  is Boltzmann’s constant, and  $T$  is the temperature. Forst and Prasil found an approximate expression for the density of states as a function of energy:

$$N(E) = Q(\beta^*) \exp(\beta^* E) / \sqrt{2\pi(\partial^2 Q(\beta) / \partial \beta^2)_{\beta=\beta^*}}, \quad (5)$$

where  $\beta^*$  is calculated by iteratively solving:

$$(\partial \ln Q(\beta) / \partial \beta)_{\beta=\beta^*} = -E. \quad (6)$$

$\beta^*$  itself is a measure of the statistical temperature. If the assumption is made that the transition state is product-like, it is quite straightforward to write a partition function for that transition state and evaluate  $\beta^*$  for a given amount of available energy. While in theory variationally optimizing the transition state should improve the value of  $\beta^*$ , in practice

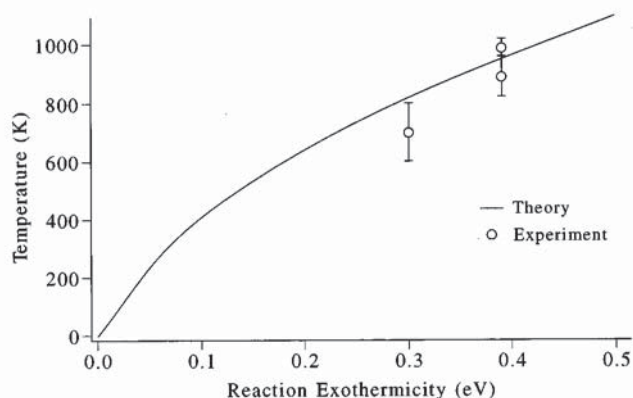


FIG. 6. Theoretical curve of product temperature versus the exothermicity of the reaction. Also plotted are the experimental measurements of OD rotational distributions. Error bars are the uncertainties in temperature obtained from the Boltzmann plots shown in Figs. 4 and 5.

the validity of such an optimization depends upon the accuracy of a well-depth estimate and assumptions about the reaction coordinate. Figure 6 shows a theoretical curve of product temperature versus the available energy, i.e., the exothermicity of the reaction. Also plotted are the experimental measurements of OD rotational distributions. The theory predicts a temperature of 800 K for the reaction of  $\text{ND}_3^+(\nu_2=0)$  and 940 K for the reaction of  $\text{ND}_3^+(\nu_2=1)$ ; the agreement with experiment is quite good.

When comparing the results of our experiment with those of others, it is important to bear in mind that our translational energies are thermal, whereas other experiments do not reach translational energies that are truly thermal. In an early study of reaction (2a), Chupka and Russell<sup>7</sup> found that the rate of reaction was insensitive to the amount of vibrational energy in the reactant  $\text{ND}_3^+$ , and interpreted the result as evidence that the reaction did not proceed through a long-lived complex. In more recent studies, however, Kemper *et al.*<sup>11</sup> found that the cross section of reaction (2a) decreases with increasing internal energy in the ion reactant. The endothermic (0.47 eV for the hydrogen isotope) channel (2b) observed by these researchers, and by Anicich, Kim and Huntress,<sup>8</sup> is not accessible at energies of our experiment. Adams *et al.*<sup>10</sup> found a rate constant of less than  $3 \times 10^{-11} \text{ cm}^3/\text{s}$  for reaction (2a). This decreased rate constant is consistent with internal excitation of the ion reactant at their 70 eV electron impact energies; however, it is surprising that they observed channel (2a) to be 100% of their product distribution. Chesnavich and Bowers<sup>9</sup> have done a statistical phase space calculation on the vibrational energy dependence of reaction (2a). They find that the cross section for reaction decreases as a function of vibrational energy in the  $\text{NH}_3^+$  reactant. No product rotational distributions from the PST calculation were reported. Chesnavich and Bowers conclude on the basis of the experimental results of Chupka and Russell<sup>7</sup> that the reaction is not statistical because the expected dependence on vibrational excitation was not observed. The subsequent results of Kemper *et al.*, however,

contradict this conclusion because they find such a decrease in the cross section.

Our results and their excellent agreement with the prediction from an RRKM-type model provide evidence that reaction does indeed proceed statistically at thermal translational energies. This result is somewhat surprising given the expectation that the well is shallow;<sup>9</sup> however, it may mean that the redistribution of internal energy proceeds rapidly or that at low translational energies internal energy redistribution can occur during traversal of a large portion of the reaction coordinate.

## ACKNOWLEDGMENTS

The authors would like to thank John J. Roberts and Kelley B. Herndon for valuable time spent on the project, Michael A. Everest for aid in running Gaussian calculations, and William R. Simpson, Hongkun Park, and Rainer A. Dressler for valuable insights. The authors are particularly grateful to Jinchun Xie for his frequent insights into experimental difficulties and constructive suggestions. This project was funded by the Air Force Office of Scientific Research under Grant No. F49620-92-J-0074-P00004.

<sup>1</sup>M. T. Bowers, *Gas Phase Ion Chemistry*, 1st ed. (Academic, New York, 1979).

<sup>2</sup>M. Baer and C.-Y. Ng, *State-Selected and State-to-State Ion-Molecule Reaction Dynamics*, 1st ed. (Wiley, New York, 1992).

<sup>3</sup>A. Fujii, T. Ebata, and M. Ito, *J. Chem. Phys.* **88**, 5307 (1988).

<sup>4</sup>W. E. Conaway, R. J. S. Morrison, and R. N. Zare, *Chem. Phys. Lett.* **113**, 429 (1985).

<sup>5</sup>H. W. Cruse, P. J. Dagdigian, and R. N. Zare, *Faraday Discuss. Chem. Soc.* **55**, 277 (1973).

<sup>6</sup>J. Xie and R. N. Zare, *J. Chem. Phys.* **96**, 4293 (1992).

<sup>7</sup>W. A. Chupka and M. E. Russell, *J. Chem. Phys.* **48**, 1527 (1968).

<sup>8</sup>V. G. Anicich, J. K. Kim, and J. W. T. Huntress, *Int. J. Mass Spectrom. Ion Phys.* **25**, 433 (1977).

<sup>9</sup>W. J. Chesnavich and M. T. Bowers, *Chem. Phys. Lett.* **52**, 179 (1977).

<sup>10</sup>N. G. Adams, D. Smith, and J. F. Paulson, *J. Chem. Phys.* **72**, 288 (1980).

<sup>11</sup>P. R. Kemper, M. T. Bowers, D. C. Parent, G. Mauclair, R. Derai, and R. Marx, *J. Chem. Phys.* **79**, 160 (1983).

<sup>12</sup>S. L. Anderson, D. M. Rider, and R. N. Zare, *Chem. Phys. Lett.* **93**, 11 (1982).

<sup>13</sup>W. E. Conaway, T. Ebata, and R. N. Zare, *J. Chem. Phys.* **87**, 3453 (1987).

<sup>14</sup>M. J. Bronikowski, Ph.D. thesis, Stanford University, 1992.

<sup>15</sup>W. K. Bischel, D. J. Bamford, and L. E. Jusinski, *Appl. Opt.* **25**, 1215 (1986).

<sup>16</sup>M. G. Sastry and K. R. Rao, *Indian J. Phys.* **24**, 27 (1941).

<sup>17</sup>C. H. Greene and R. N. Zare, *J. Chem. Phys.* **78**, 6741 (1983).

<sup>18</sup>R. Altkorn and R. N. Zare, *Annu. Rev. Phys. Chem.* **35**, 265 (1984).

<sup>19</sup>W. Demtröder, *Laser Spectroscopy* (Springer-Verlag, Berlin, 1988), 3rd ed.

<sup>20</sup>W. L. Dimpfl and J. L. Kinsey, *J. Quant. Spectrosc. Radiat. Transfer* **21**, 233 (1979).

<sup>21</sup>M. A. A. Clyne, J. A. Coxon, and A. R. W. Fat, *J. Mol. Spectrosc.* **46**, 146 (1973).

<sup>22</sup>P. Andresen, G. S. Ondrey, and B. Titze, *J. Chem. Phys.* **80**, 2548 (1984).

<sup>23</sup>P. Andresen and R. Schinke, in *Molecular Photodissociation Dynamics*, edited by M. N. R. Ashfold (The Royal Society of Chemistry, London, 1987), Vol. 1, p. 243.

<sup>24</sup>M. R. Nyden and G. A. Petersson, *J. Chem. Phys.* **75**, 1843 (1981).

<sup>25</sup>G. A. Peterson, A. Bennet, T. G. Tensfeldt, M. A. Al-Laham, W. Shirley, and J. Mantzaris, *J. Chem. Phys.* **84**, 2193 (1988).

<sup>26</sup>G. A. Peterson, T. Tensfeldt, and J. A. Montgomery, *J. Chem. Phys.* **94**, 6091 (1991).

<sup>27</sup>G. A. Peterson and M. A. Al-Laham, *J. Chem. Phys.* **94**, 6081 (1991).

- <sup>28</sup>J. A. Montgomery, J. W. Ochterski, and G. A. Petersson, *J. Chem. Phys.* **101**, 5900 (1994).
- <sup>29</sup>M. J. Frisch, G. W. Trucks, H. B. Schlegel, P. M. W. Gill, B. G. Johnson, M. A. Robb, J. R. Cheeseman, T. Keith, G. A. Petersson, J. A. Montgomery, K. Raghavachari, M. A. Al-Laham, V. G. Zakrzewski, J. V. Ortiz, J. B. Foresman, J. Cioslowski, B. B. Stefanov, A. Nanayakkara, M. Challacombe, C. Y. Peng, P. Y. Ayala, W. Chen, M. W. Wong, J. L. Andres, E. S. Replogle, R. Gomperts, R. L. Martin, D. J. Fox, J. S. Binkley, D. J. Defrees, J. Baker, J. P. Stewart, M. Head-Gordon, C. Gonzalez, and J. A. Pople, *GAUSSIAN 94*, Revision B.1 (Gaussian, Pittsburgh, PA, 1995).
- <sup>30</sup>O. K. Rice and H. C. Ramsperger, *J. Am. Chem. Soc.* **49**, 1617 (1927).
- <sup>31</sup>L. S. Kassel, *J. Phys. Chem.* **32**, 225 (1928).
- <sup>32</sup>O. K. Rice and H. C. Ramsperger, *J. Am. Chem. Soc.* **50**, 617 (1928).
- <sup>33</sup>L. S. Kassel, *Kinetics of Homogeneous Gas Reactions* (Chemical Catalog Co., New York, 1932).
- <sup>34</sup>R. A. Marcus and O. K. Rice, *J. Phys. Colloid Chem.* **55**, 894 (1951).
- <sup>35</sup>R. A. Marcus, *J. Chem. Phys.* **20**, 359 (1952).
- <sup>36</sup>W. Forst and Z. Prásil, *J. Chem. Phys.* **51**, 3006 (1969).
- <sup>37</sup>P. J. Robinson and K. A. Holbrook, *Unimolecular Reactions* (Wiley-Interscience, New York, 1972).
- <sup>38</sup>W. Forst, *Theory of Unimolecular Reactions* (Academic, New York, 1973).
- <sup>39</sup>R. G. Gilbert and S. C. Smith, *Theory of Unimolecular and Recombination Reactions* (Blackwell Scientific, Oxford, 1990).
- <sup>40</sup>K. A. Holbrook, M. J. Pilling, and S. H. Robertson, *Unimolecular Reactions*, 2nd ed. (Wiley, New York, 1996).